Palaeobiodiversity and Palaeoenvironments (2025) 105:129–146
https://doi.org/10.1007/s12549-025-00642-9

SENCKENBERG

ORIGINAL PAPER

Lower and middle Famennian (Upper Devonian) conodont biostratigraphy from Compte section (Central Pyrenees, Spain)

Héctor Barrera-Lahoz[1] · José Ignacio Valenzuela-Ríos[2,3] · Jau-Chyn Liao[3]

Received: 17 July 2024 / Revised: 22 September 2024 / Accepted: 28 January 2025 / Published online: 15 April 2025

Abstract

A detailed analysis of the conodont sequence in the Compte section, located in the Spanish Central Pyrenees, demonstrates an almost continuous biostratigraphical record for the Famennian sequence studied. Forty-seven conodont taxa have been identified allowing the identification of six lower and middle Famennian zones through the index taxa. The lower part of the section, corresponding to the Comabella Formation, begins with the *Palmatolepis termini* Zone, followed by the *Palmatolepis glabra prima* Zone. The top of the Comabella Formation comprises the *Palmatolepis gl. pectinata* Zone with the *Palmatolepis rhomboidea* Zone starting near the base of the La Mena Formation. At the middle of this formation the *Palmatolepis gracilis gracilis* Zone appears, and near the top, the *Palmatolepis marginifera marginifera* Zone marks the beginning of the middle Famennian, which continues through the base of the Barousse Formation. Comparing these new findings with the previous data from Boersma (1973) reveals significant chronostratigraphic and biostratigraphic discrepancies, which are discussed in detail. Additionally, comparisons with other sequences located worldwide show that the ranges of most conodonts appear delayed in the Compte section. Our data supports the revised global standard conodont zonation proposed by Spalletta et al. (2017) for this portion of the Famennian.

Keywords Upper Devonian · Lower–middle Famennian boundary · Conodont biostratigraphy · Spanish Central Pyrenees · Global standard conodont zonation

Introduction

Devonian stratigraphy in the Central Pyrenees is complex, specially for the Lower Devonian, and shows a variety of facies developments from north to south and from east to west (Fig. 1a1); they primarily constituting the sedimentary record of the Pyrenean Axial zone (Fig. 1a2), and have been described and divided into "facies area" by various authors (Mey 1967a, b; Hartevelt 1970; Zwart 1979). These facies-area include the North Pyrenean, Northern, Central, Western and Southern. The latter has been further subdivided into four subfacies-area: Renanué, Baliera, Sierra Negra and Compte (Mey 1967a; Zwart 1979; Valenzuela-Ríos and Liao 2006) (Fig. 1b). The Compte subfacies comprises the western area, known as the Nogueras Zone, (to which the studied section belongs), and the eastern area, called the Cadí Nape (Sanz-López 1995) (Fig. 1b). The arrangement and correlation of all stratigraphic units across the Pyrenees requires precise chronological tools. Conodont sequences serve as the most effective tool in these rocks, making Devonian conodont-based biostratigraphic research fundamental and highly relevant.

Detailed biostratigraphic works on the Lower and Middle Devonian of the Compte subfacies-area, (Liao and Valenzuela-Ríos 2008; 2013; Martínez-Pérez et al. 2011; Gouwy et al. 2013; Valenzuela-Ríos and Liao 2012; 2024; Valenzuela-Ríos et al. 2015; Slavík et al. 2016) have

This article is a contribution to the special issue "Special contributions in honour of Peter Königshof"

✉ Héctor Barrera-Lahoz
699926@unizar.es

José Ignacio Valenzuela-Ríos
Jose.I.Valenzuela@uv.es

Jau-Chyn Liao
jaucliao@ucm.es

[1] Department of Earth Sciences, University of Zaragoza, C/ Pedro Cerbuna 12, 50009 Zaragoza, Spain

[2] Department of Botany and Geology, University of Valencia, C/ Dr. Moliner 50, 46100 Burjasot, Spain

[3] Department of Geodynamic, Stratigraphy and Paleontology, University Complutense of Madrid, C/ José Antonio Novais 12, 28040 Madrid, Spain

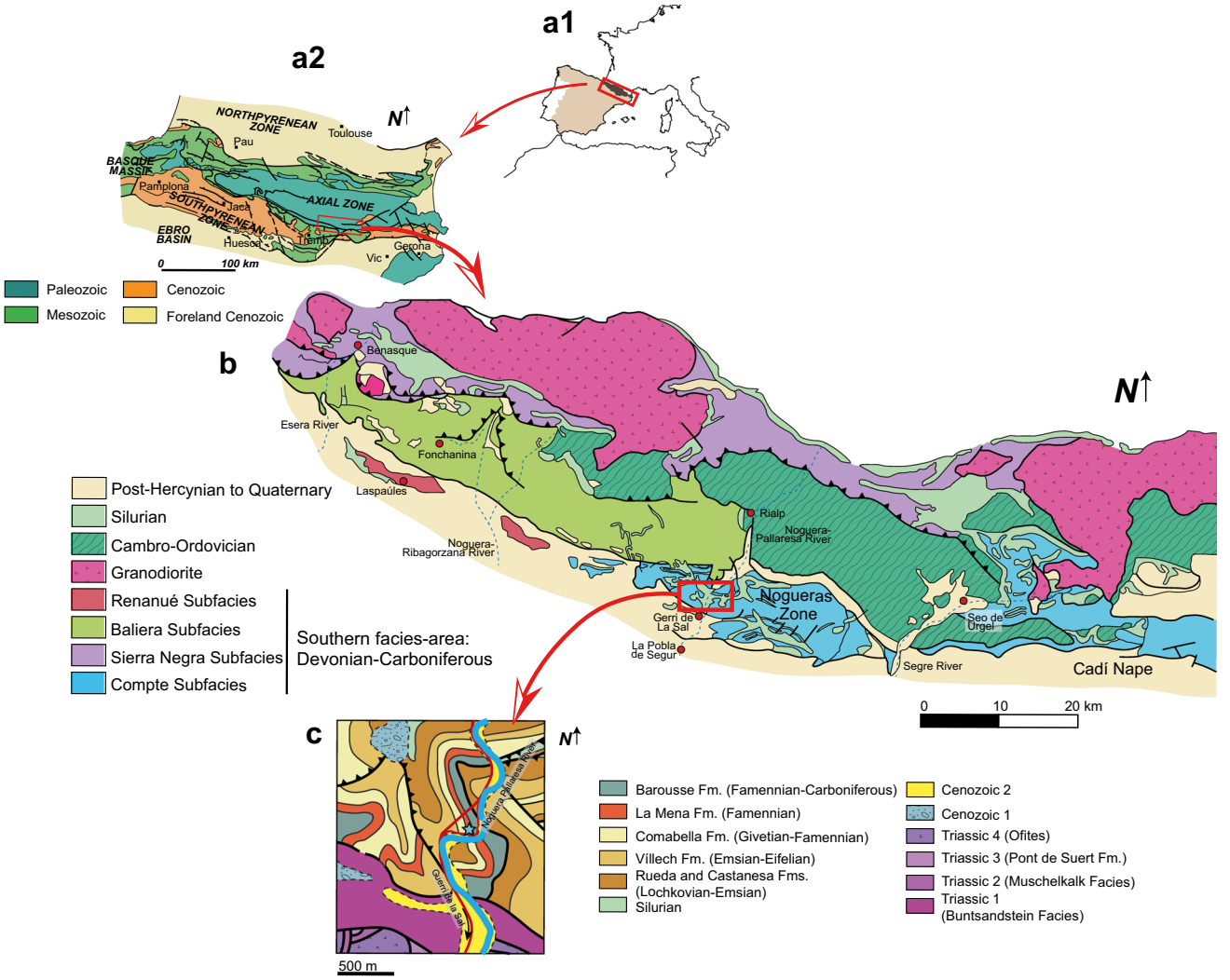

Fig. 1 Geographical and geological setting of the Compte section. **a1** Geographic setting of the Pyrenees in Western Europe Zone. **a2** Structural map of the Pyrenees (modified from Barnolas and Pujalte, 2004). **b** Geological and southern-facies map of the Central Pyrenees area (modified from Valenzuela-Ríos et al. 2015). **c** Geological map of Compte section zone, blue star represents the studied Compte section (modified from Institut Cartogràfic I Geològic de Catalunya, 2023)

been conducted in the Nogueras Zone. In contrast, the Frasnian–Famennian transition has received less attention (Sánchez de Posada et al. 2008; Silvério et al. 2021). Additionally, Frasnian to Carboniferous rocks of the Compte subfacies-area have been investigated in the eastern side of the Central Pyrenees, in the Cadí Nape (Fig. 1b), (Sanz-López 1995).

Liao and Valenzuela-Ríos 2017 and Valenzuela-Ríos et al. 2017 presented preliminary reports on Famennian conodonts in different Pyrenean sections. However, an exhaustive analysis on Famennian conodont biostratigraphy is still lacking. The Compte section, in particular, yields an almost continuous Givetian to Tournaisian conodont record, which has been the subject of extensive research in the last decades (Liao and Valenzuela-Ríos 2008; 2013; Gouwy et al. 2013). Pioneer conodont studies reported the presence of Middle Devonian to lower Carboniferous conodonts (Ziegler 1959), with Boersma (1973) providing an initial conodont-based zonation for this interval. Subsequent studies by Liao and Valenzuela-Ríos (2008) focused on detailed Givetian and early Frasnian high-resolution biostratigraphy. Recently, Silvério et al. (2021) analysed the Frasnian–Famennian boundary and Barrera-Lahoz et al. (2024) described the lower and middle Famennian conodont record.

Despite these studies, a detailed Famennian biostratigraphy of the Compte section remains to be completed.

Famennian rocks in this and nearby areas are grouped into three lithological units: the Comabella, La Mena and Barousse Formations, which roughly correspond to the former Compte A, B and C units, respectively. The contact between the Comabella and La Mena formations is diachronous in this area (Valenzuela-Ríos and Liao 2006); consequently, the biostratigraphical characterisation of the Compte section and its correlation with other sections is instrumental in deciphering the Famennian history of the Pyrenean records.

Our main purpose is to identify and characterise the lower and middle Famennian conodont biostratigraphy in the Compte section with high resolution, with special focus on the La Mena Formation and to discuss the Pyrenean ranges globally. Additionally, we compare our results with the data from Boersma (1973). We also discuss the possible position of Nehden and Condroz Global Events during the lower–middle Famennian in the Compte section and their effects in the conodont record.

Material provenance and methods

Boersma (1973: fig. 6) initially studied the Compte section, assigning these rocks to the Compte Formation and identifying three members (A, B, and C). These members correspond to the current Comabella, La Mena, and Barousse formations, respectively (Fig. 1c). The Comabella Formation in the Compte section spans from the Givetian through the early Famennian; the La Mena Formation is early to middle Famennian in age, and the Barousse Formation extends into the early Carboniferous (Liao and Valenzuela-Ríos 2017). The Comabella Formation consists of well-bedded and locally nodular limestones with grey, dark, pink, and green colours. The La Mena Formation is composed of red (pseudo)nodular "griotte" limestones, purple bedded limestones, and grey and red nodular limestones. Pink and grey nodular limestones characterise the Barousse Formation.

The studied part of the Compte section is located 16 km north of La Pobla de Segur (42°20'14.2"N, 1°04'04.5"E). The Devonian rocks in this section are inverted and contact tectonically with Triassic rocks by faults (Fig. 1c). The studied section is 11.73 m thick (Fig. 2) and includes the uppermost 4.53 m of the Comabella Formation (beds 98 to 105), approximately 5.75 m of the La Mena Formation (beds 106 to 116), and the basal 1.45 m of the Barousse Formation (beds 117 to 120). The detailed lithologic succession of the studied part of the Compte section comprises different types of limestone, which from base up are as follows:

- **Basal Part, Upper part of Comabella Formation** (Beds 98–99, Figs. 3a, d): 1.63 m of grey, massive limestone that becomes irregular and nodular with pink traces upwards.
- **Uppermost Comabella Formation** (Beds 100–105, Figs 3b, h): 2.90 m of well-bedded and irregular bedding grey limestone with few shale layers. Near the top, in Bed 105, the limestone turns dark-grey, argillaceous, and brecciated.
- **Basal La Mena Formation** (Beds 106–111 Figs. 3b, e): 1.62 m of "griotte" red nodular limestone with irregular geometry, containing macrofossils like orthoceratids and ammonoids.
- **Overlaying Limestone** (Bed 112): 2.4 m of well-bedded to massive purple limestone with some grey layers.
- **Upper La Mena Formation** (Beds 113–116 Figs. 3c, g, i): 1.73 m of red nodular limestone with scarce cephalopods, turning into ochre in the base and purple and grey nodular limestone near the top.
- **Basal Barousse Formation** (Beds 117–120, Figs. 3c, f): 1.45 m of pink and grey nodular limestone, passing to fully light grey limestone.

Fifty limestone samples were collected from the upper part of the Comabella Formation, the La Mena Formation, and the lowermost part of the Barousse Formation in the Compte section (Fig. 2). The mean sample weight ranged from 0.5 to 0.6 kg, with a minimum of 0.025 kg and a maximum of 2.85 kg (Tables 1, 2, 3). The samples were dissolved using acetic or formic acids (~7–8%) in 5–10 liters of water solutions; the residues were washed by decantation and subsequently dried in oven at approximately 60 ºC. Conodont fossil elements were picked out using a LEICA Wild M3B microscope. Selected specimens were photographed using a Scanning Electron Microscope (Hitachi S4800) at the University of Valencia. Sample richness varied, with between 5 to 153 conodont elements per sample, yielding a total of 2402 complete and incomplete Pa respective I conodont elements. The state of preservation is variable. The conodont specimens were deposited in the Department of Botany and Geology, University of Valencia.

This detailed stratigraphic and lithologic analysis of the Compte section provides crucial data for understanding the Famennian history and conodont biostratigraphy of the Pyrenean records.

Biostratigraphy

Ziegler (1962a) established the Famennian conodont zonation based on records from the Rhenish Slate Mountains, originally composed of seven conodont zones: *Palmatolepis triangularis*, *Palmatolepis crepida*, *Palmatolepis*

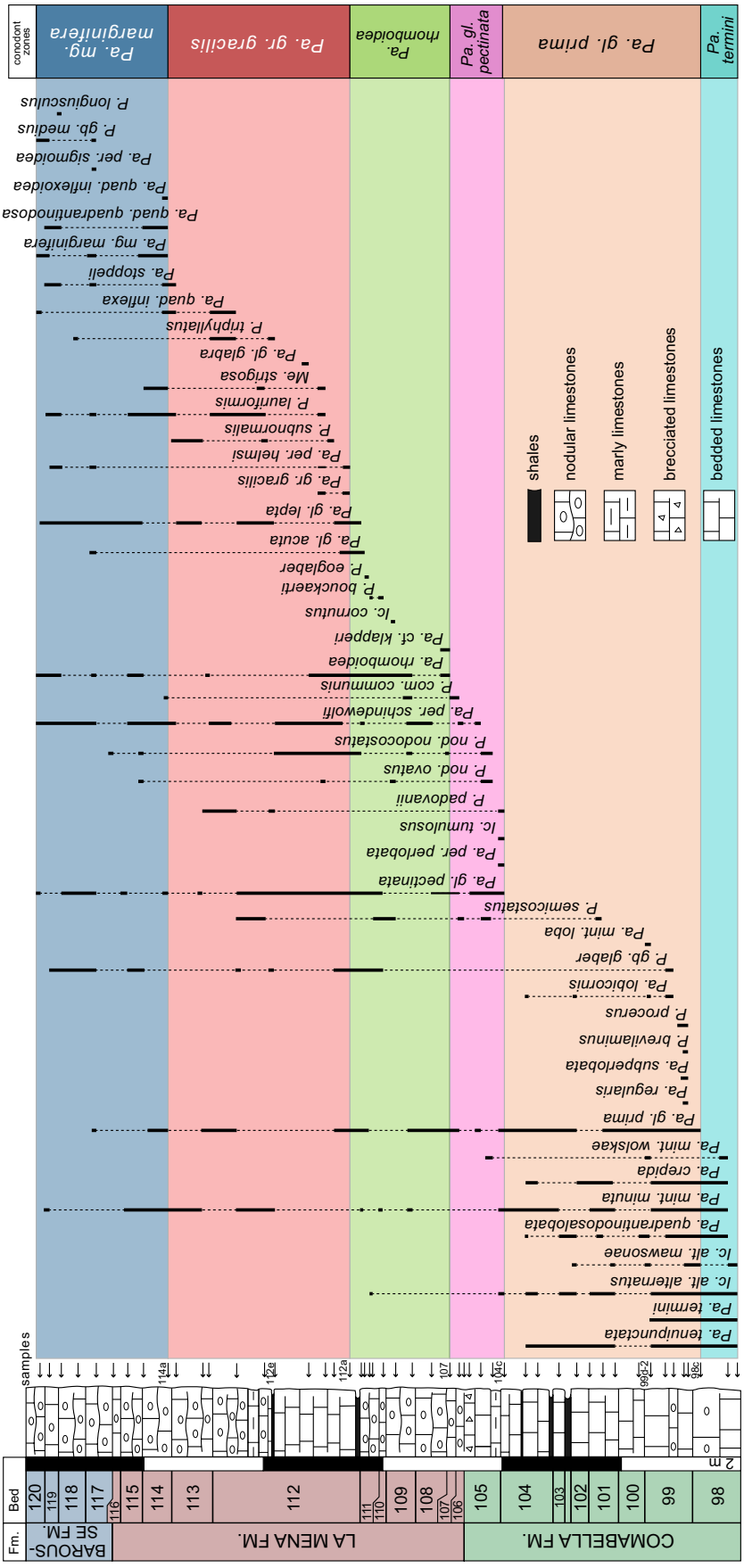

Fig. 2 Lithological, stratigraphical and biostratigraphical column of the Compte section. The continuous line represents a continuous range of the conodont taxa and discontinuous line represents no taxa recorded. The ranges of *Palmatolepis gl. prima* and *Pa. gl. lepta* includes all of their morphotypes ranges. Arrows represent each taken sample. *Pa.*: *Palmatolepis*; *P.*: *Polygnathus*; *Ic.*: *Icriodus*; *Me.*: *Mehlina*

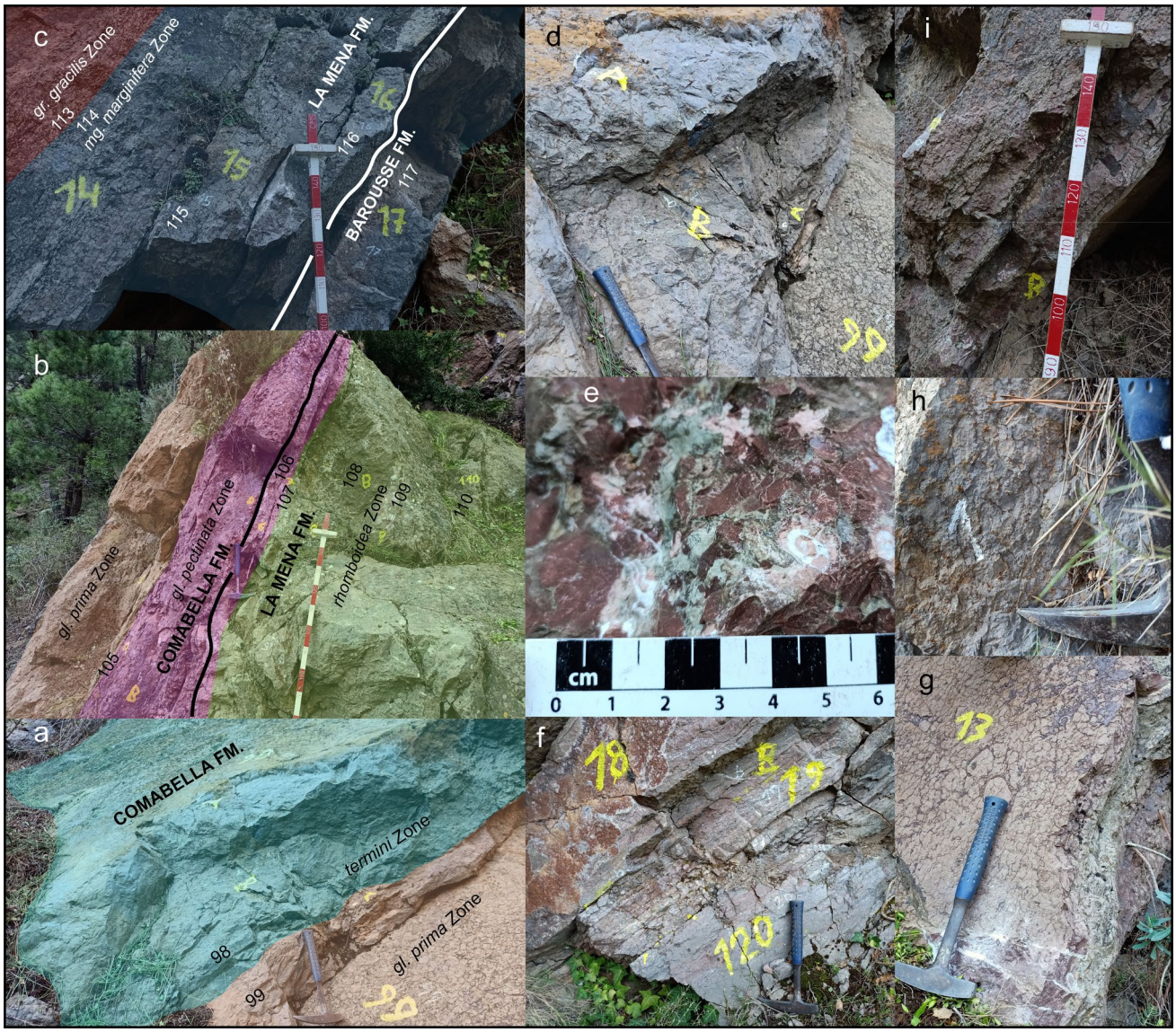

Fig. 3 Field views of the Compte section and conodont zones. **a** Comabella Fm. and *Palmatolepis termini–gl. prima zones* zones. 98 to 99. numbers represent Beds 98 to 99. **b** Comabella and La Mena Fms. boundary and *Palmatolepis gl. prima–rhomboidea* zones. **c** La Mena and Barousse Fms. boundary and *Palmatolepis gr. gracilis–mg. marginifera* zones **d** Comabella Fm. grey massive layers of Beds 98–99. **e** Red nodular griotte limestone detail with nautiloid fossil of La Mena Fm., Bed 109. **f** Pink and grey nodular limestones of Barousse Fm., Beds 118–120. **g** Red and ochre nodular limestones of La Mena Fm., base of Bed 113. **h** Light grey bedded limestones of Comabella Fm. Bed 101. **i.** Grey and purple nodular limestones of La Mena Fm., Bed 114

rhomboidea, *Palmatolepis quadrantinodosa*, *Scaphignathus velifer*, *Polygnathus styriacus* and *Bispathodus costatus*. Sandberg and Ziegler (1973) later subdivided the Ziegler's *rhomboidea* Zone into Lower and Upper *rhomboidea* zones, based on the First Appearance Datum (FAD) of *Palmatolepis rhomboidea* and *Palmatolepis gracilis gracilis* respectively. Ziegler and Sandberg (1984) then replaced the Ziegler's *Palmatolepis quadrantinodosa* Zone into Early and Late *Palmatolepis marginifera* zones, defined by the FAD of *Palmatolepis marginifera marginifera* and *Palmatolepis marginifera utahensis* correspondingly.

In 1990, Ziegler and Sandberg further refined the Late Devonian Standard Conodont Zonation, by subdividing the *crepida* Zone into Lower, Middle, Upper and Uppermost *crepida* zones. The base of the Lower *crepida* Zone was defined by the FAD of *Palmatolepis crepida*. The Middle *crepida* Zone begins with the FAD of *Palmatolepis termini*, the Upper *crepida* Zone with the FAD of *Palmatolepis glabra prima,* and the Uppermost *crepida* Zone with the FAD of *Palmatolepis glabra pectinata*. Spalletta et al. (2017) redefined this global standard conodont zonation for the Famennian Stage, with the designation of new zones

Table 1 Numerical distribution of pectiniform conodont specimens record from Beds 98 to 104, including sample names, conodont biozones extension, formations and sample weight

Formation	Comabella															
Conodont zones	*Pa. termini*		*Pa. gl. prima*													
Sample name	CP/98a	CP/98b	CP/98c	CP/99a	CP/99b	CP/99c	CP/99d-1	CP/99d-2	CP/100	CP/101a	CP/101b	CP/102a	CP/102b	CP/103	CP/104a	CP/104b
Sample weight (kg)	0.41	0.65	0.73	0.455	0.53	0.75	0.4	1.275	0.56	0.75	0.59	0.455	0.58	0.47	0.595	0.585
Pa. tenuipunctata	1	2	17	12	5	7	2	9		8	2	2	3	2	4	7
Pa.* cf. *tenuipunctata			3		2	2			1	1		1			2	
Pa.* cf. *quadrantinodosalobata	3				1			2			3				1	4
Pa. quadrantinodosalobata		5	10	5	2	1		4	1		3		2	2		8
Pa. minuta minuta		4	2	2	1	4	1	4		5	2	2		1	3	4
Pa. crepida		4	4	4	4	6	4	19		8	2	3	5		3	32
Pa. termini	1	5	8	9	4	9	1	10								
Pa. glabra prima			25	15	4	20	7	18	3	10	2		3	5	8	34
Pa. glabra* cf. *prima			1			1	1	4		1		1				
Pa. regularis				2												
Pa. subperlobata				2	1											
Pa.* cf. *subperlobata				1												
Pa. lobicornis						2		1					1			1
Pa.* cf. *lobicornis								1								
Pa. minuta wolskae		1						1								
Pa. minuta loba								1								
***Palmatolepis* sp. Indet.**	13	8	72	26	11	29	13	32	3	26	20	13	12	12	21	57
Ic. alternatus alternatus	1	4	1	1	14	2	1	3		1	11		2		2	
Ic.* cf. (*alternatus*) *alternatus					4	1				1	1		3		2	
Ic. alternatus mawsonae	1		1	3	4			5			2		2			
***Icriodus* sp. Indet.**	2	3	1		2	1	1	5			5	2	10	5	2	1
P. brevilaminus				1												
P. procerus				4	2											
P. semicostatus											1					
P. glaber glaber						2										
***Polygnathus* sp. Indet.**	1		4	12	2	2		1	1	2	4	1	5	2		2

Table 2 Numerical distribution of pectiniform conodont specimens record from Beds 104 to 112, including sample names, conodont biozones extension, formations and sample weight

Formation	Comabella					La Mena																	
Conodont zones	*Pa. gl. pectinata*					*Pa. rhomboidea*												*Pa. gr. gracilis*					
Sample name	CP/1 04c	CP/1 05a	CP/1 05b	CP/1 05c	CP/1 05d	CP/1 06	CP/1 07	CP/1 08	CP/1 09a	CP/1 09b	CP/1 10	CP/1 11a-1	CP/1 11a-2	CP/1 11b	CP/1 11c	CP/1 12a	CP/1 12b	CP/1 12c	CP/1 12d	CP/1 12e	CP/1 12f	CP/1 12g
Sample weight (kg)	0.645	1.255	0.735	0.52	0.61	0.53	0.49	0.57	0.52	0.485	0.565	0.59	0.025	0.56	0.715	1.13	0.665	0.95	0.56	0.69	0.465	0.72
Pa. minuta minuta	1								1		3				2					4	3	1
Pa. glabra prima	4		1			3	2	3	1				1	3	1	1	3					2
Pa. glabra* cf. *prima	1						2															
Pa. minuta wolskae		1	1																			
Pa. perlobata perlobata	1																					
Pa. glabra pectinata	2	1	6	2		5	3	3			2	2	1	6	4	3	5	2	1	5	1	3
Pa. perlobata schindewolfi			1		1	1		1	6					1		2	2	2	1	2		5
Pa. perlobata* cf. *perlobata				1																		
Pa. rhomboidea							1		2	2	13	5	8	3	4	12	15	15	3			
Pa.* cf. *klapperi							1															
Pa. glabra acuta														1	1	2	3					
Pa. glabra lepta															1	1	3			1	1	1
Pa. gracilis gracilis																1		1				
Pa. perlobata helmsi																1		1				
Pa. glabra glabra																			1			
Pa. quadrantinodosa inflexa																						2
***Palmatolepis* sp. Indet.**	8	2	8	2	1	7	9	5	4	1	4	6	4	16	18	13	6	12	5	12	5	7
Ic. alternatus alternatus	5											1										
Ic.* cf. (*alternatus*) *alternatus												1										
Ic. tumulosus	3																					
Ic. cornutus										1												
***Icriodus* sp. Indet.**	16	2								3												
P. semicostatus		7	4		1	5				1	4	3									1	1
P. padovanii	1																			2		2
P. nod. nodocostatus		1	1				1		2						1	1	1	3	1	1		
P. nod.* cf. *nodocostatus								1	1						1					1		
P. nod. ovatus		4	1						1									1				
Po. communis communis						1	1		1													
P. glaber glaber											2	2	1	1	2	5	4			2		2
P. bouckaerti											1	1										
P. eoglaber													1	1								
P. subnormalis																	1				1	
P. triphyllatus																				3		1
P. lauriformis																		1			2	5
***Polygnathus* sp. Indet.**	8	13	2	11	2	23		5	9	1	9	4	3	15	5	5	3	5	2	6	5	7
Me. strigosa																		1			1	

Table 3 Numerical distribution of pectiniform conodont specimens record from Beds 113 to 120, including sample names, conodont biozones extension, formations and sample weight

Formation	La Mena							Barousse				
Conodont zones	*Pa. gr. gracilis*			*Pa. mg. marginifera*								
Sample name	CP/113a	CP/113b	CP/113c	CP/114a	CP/114b	CP/115	CP/116	CP/117	CP/118a	CP/118b	CP/119	CP/120
Sample weight (kg)	0.465	0.525	0.565	0.725	1.01	0.74	0.415	2.875	1	0.64	0.7	0.5
Pa. minuta minuta		1	4	28	3	1					1	
Pa. glabra prima	1	2		3	3			4				
Pa. glabra pectinata		1		7		2		17	1	1		2
Pa. perlobata schindewolfi	1		2	5	1	1		3	1	1	1	1
Pa. rhomboidea	1				4	12		10		7	10	2
Pa. glabra acuta								1				
Pa. glabra lepta		3	1		38	8	1	4	9	13	6	3
Pa. perlobata helmsi								3			3	
Pa. quadrantinodosa inflexa	1		1	1								1
Pa. stoppeli			1	4				2		2	1	
Pa. quadrantinodosa inflexoidea				1								
Pa. quadrantinodosa quadrantinodosa				2	3					1	1	
Pa. marginifera marginifera				1	1	3		6			3	2
Pa. perlobata sigmoidea								1				
***Palmatolepis* sp. Indet.**	8	6		14	47	26	6	71	24	35	14	20
P. padovanii	2	2										
P. nod. nodocostatus					1		1					
P. nod.* cf. *nodocostatus			1					3	1		1	
P. nod. ovatus					1							
P. communis communis				1								
P. glaber glaber					1	1		6	1	1	2	
P. subnormalis		1	2									
P. triphyllatus	2			1					1			
P. lauriformis	4		4	12	5	3		1		3	1	
P.* cf. *lauriformis				2								
P. glaber medius								3			4	1
P. longiusculus										1		
***Polygnathus* sp. Indet.**	6	4	1	15	5	2	1	18	1	3	5	4
Me. strigosa				2	1							

named after their index taxa, an approach followed in this study.

The formal establishment of the base of the Famennian stage has been long debated. In 1989 and 1993, the Subcommission on Devonian Stratigraphy (SDS) proposed aligning the base of the Lower *triangularis* Zone with the Global Boundary Stratotype Section and Point (GSSP) for the base of the Famennian, defined by the FAD of *Palmatolepis triangularis*. The reintroduction of *Palmatolepis ultima* as a discrete species and the restriction of the concept of *Palmatolepis triangularis* to the holotype description led to a reinterpretation of the Lower *triangularis* Zone (Klapper et al. 2004). Klapper (2007) emphasise the acme of *Palmatolepis ultima* immediately above the upper Frasnian extinction event and the record of *Palmatolepis subperlobata*, which characterises the base of *subperlobata* Zone and the base of the Famennian Stage. The FAD of *Palmatolepis subperlobata* now marks the base of the *triangularis* Zone and of the Famennian stage (Becker et al. 2012; Spalletta et al. 2017). Furthermore, there were proposals for the subdivision of the Famennian into four substages: lower, middle, upper and uppermost (Schülke et al. 2003; Marshall 2005).

The conodont fauna in the studied part of the Compte section consists of 47 taxa (Tables 1, 2, 3) belonging to four genera (Barrera-Lahoz et al. 2024). The presence of the index taxa allows the recognition of six successive lower to middle Famennian conodont zones, from the *Palmatolepis termini* Zone to *Palmatolepis mg. marginifera* Zone (Figs. 2–3). This detailed biostratigraphic framework provides critical insights into the Famennian conodont biostratigraphy in the Central Pyrenees contributing to a better understanding of the global conodont zonation and its regional implications.

Famennian Conodont Zonation in the Compte Section

Palmatolepis termini Zone

The presence of *Palmatolepis termini* (Figs. 4a–b) in the lowest sample of the studied part of the Compte section (CP/98a), below the entry of *Palmatolepis glabra prima* (sample CP/98c) allows the recognition of the *termini*

Zone. However, in the recent review of unpublished material from Silvério et al. 2021, this zone starts below Bed 98. Other conodonts recorded in sample CP/98a include *Palmatolepis tenuipunctata* (Fig. 4d), *Icriodus alternatus alternatus* (Figs. 4o–p) and *Icriodus alt. mawsonae* (Figs. 4n, q). Slightly higher in the section (sample CP/98b), the lowest records of *Palmatolepis quadrantinodosalobata* (Fig. 4g), *Palmatolepis crepida* (Fig. 4f), *Palmatolepis minuta minuta* (Fig. 4e) and *Palmatolepis mint. wolskae* (Fig. 4k) complete the conodont assemblage of the *termini* Zone.

Palmatolepis glabra prima Zone

The base of the *Palmatolepis gl. prima* Zone is defined by the entry of *Palmatolepis glabra prima* (morphotype 1) (Fig. 4c) near the top of Bed 98 (sample CP/98c) (Fig. 3a). This zone extends to the upper boundary of Bed 104 (sample CP/104c), which records the entry of the defining taxon of the following Zone. The lowest record of the morphotype 3 of *Palmatolepis glabra prima* is documented in sample CP/104b. All taxa recorded in the *Palmatolepis termini* Zone continue into the *Palmatolepis glabra prima* Zone. Several taxa have their highest records within this zone, including *Palmatolepis termini* (sample CP/99d-2), *Palmatolepis tenuipunctata* (sample CP/104b), *Icriodus alt. mawsonae* (sample CP/102), *Palmatolepis quadrantinodosalobata* (sample CP/104b), and *Palmatolepis crepida* (sample CP/104b). Slightly above the base of the zone (sample CP/99a) *Palmatolepis subperlobata* (Fig. 4i), *Palmatolepis regularis* (Fig. 4h), *Polygnathus brevilaminus* (Fig. 4t), and *Polygnathus procerus* (Figs. 4l–m) enter. *Palmatolepis lobicornis* (Fig. 4j) occurs 45 cm above the base of the zone (sample CP/99c) and is restricted to the *Palmatolepis glabra prima* Zone, up to Bed 104 (sample CP/104b). *Polygnathus gb. glaber* (Fig. 5p) is also identified in sample CP/99c, with a discontinuous record up to near the top of the section (Bed 119), but its only record in the *Palmatolepis glabra prima* Zone is in sample CP/99c. In sample CP/99d-2 *Palmatolepis mint. loba* appears. The entry of *Polygnathus semicostatus* (Figs. 4u–v) in sample CP/101b represents the highest entry of a taxon in this zone.

Palmatolepis glabra pectinata Zone

The base of the *Palmatolepis glabra pectinata* Zone is defined by the first record of its index taxon, *Palmatolepis gl. pectinata* (Fig. 5a), near the top of Bed 104 (sample CP/104c). This zone extends 90 cm through Bed 107, which belongs to La Mena Fm. (Fig. 3b). In addition to the index taxon, the following taxa enter at the base of the zone: *Palmatolepis perlobata perlobata* (Fig. 4x), *Icriodus tumulosus* (Fig. 4r) and *Polygnathus padovanii* (Fig. 5n). The *Polygnathus nodocostatus*-stock represented by *Polygnathus nod. nodocostatus* (Fig. 5i) and *Polygnathus nod. ovatus* (Fig. 5j) appears in Bed 105 (sample CP/105a), The following sample, CP/105b, 20 cm higher, shows the entry of *Palmatolepis per. schindewolfi* (Fig. 5w) and the last record of the morphotype 1 of *Palmatolepis gl. prima*. Slightly higher (sample CP/106), *Polygnathus communis communis* enters (Fig. 5l). Several taxa that appeared previously continue through the zone and into higher zones, including *Icriodus alt. alternatus*, *Palmatolepis mint. minuta* and *Polygnathus semicostatus*. *Polygnathus glaber glaber* is not recorded in the *Palmatolepis glabra pectinata* Zone, but below and above it (*Palmatolepis gl. prima* and *Palmatolepis rhomboidea* zones). *Palmatolepis mint. wolskae* has its highest record within the *Palmatolepis gl. pectinata* Zone (sample CP/105b).

Palmatolepis rhomboidea Zone

The lower boundary of the *Palmatolepis rhomboidea* Zone is defined by the first occurrence of *Palmatolepis rhomboidea* (Fig. 5f), which enters 9 cm above the base of Bed 107 (sample CP/107) in the Compte section. This level is 20 cm above the base of the La Mena Fm. (Fig. 3b). Together with the index taxon, the unique record of *Palmatolepis* cf. *klapperi* is documented. Higher up, the successive entries of *Icriodus cornutus* (Fig. 4s) (unique record in sample CP/109b), *Polygnathus bouckaerti* (Fig. 4w) (samples CP/110 and CP/111a-1), *Polygnathus eoglaber* (sample CP/111a-2; unique record), *Palmatolepis gl. acuta* (Fig. 5d) (sample CP/111b), and the early morphotype of *Palmatolepis gl. lepta* (Fig. 5b) (sample CP/111c) are observed. These latter two taxa continue higher. Numerous taxa from previous zones are also recorded in the *Palmatolepis rhomboidea* Zone and continue into higher zones: *Palmatolepis mint. minuta*, *Palmatolepis gl. prima*, *Polygnathus gb. glaber*, *Polygnathus semicostatus*, *Palmatolepis gl. pectinata*, *Polygnathus nod. nodocostatus*, *Polygnathus nod. ovatus*, *Palmatolepis per. schindewolfi* and *Polygnathus com. communis*. *Icriodus alt. alternatus* has its last record in this zone (Bed CP/111a-1). *Polygnathus padovanii*, which occurs in the previous zone and disappears in the following *gr. gracilis* Zone, was not recorded within the *rhomboidea* Zone in the Compte section.

Palmatolepis gracilis gracilis Zone

The lower boundary of the *Palmatolepis gracilis gracilis* Zone is defined by the first occurrence of *Palmatolepis gr. gracilis* (Figs. 5g–h) in the lower part of Bed 112

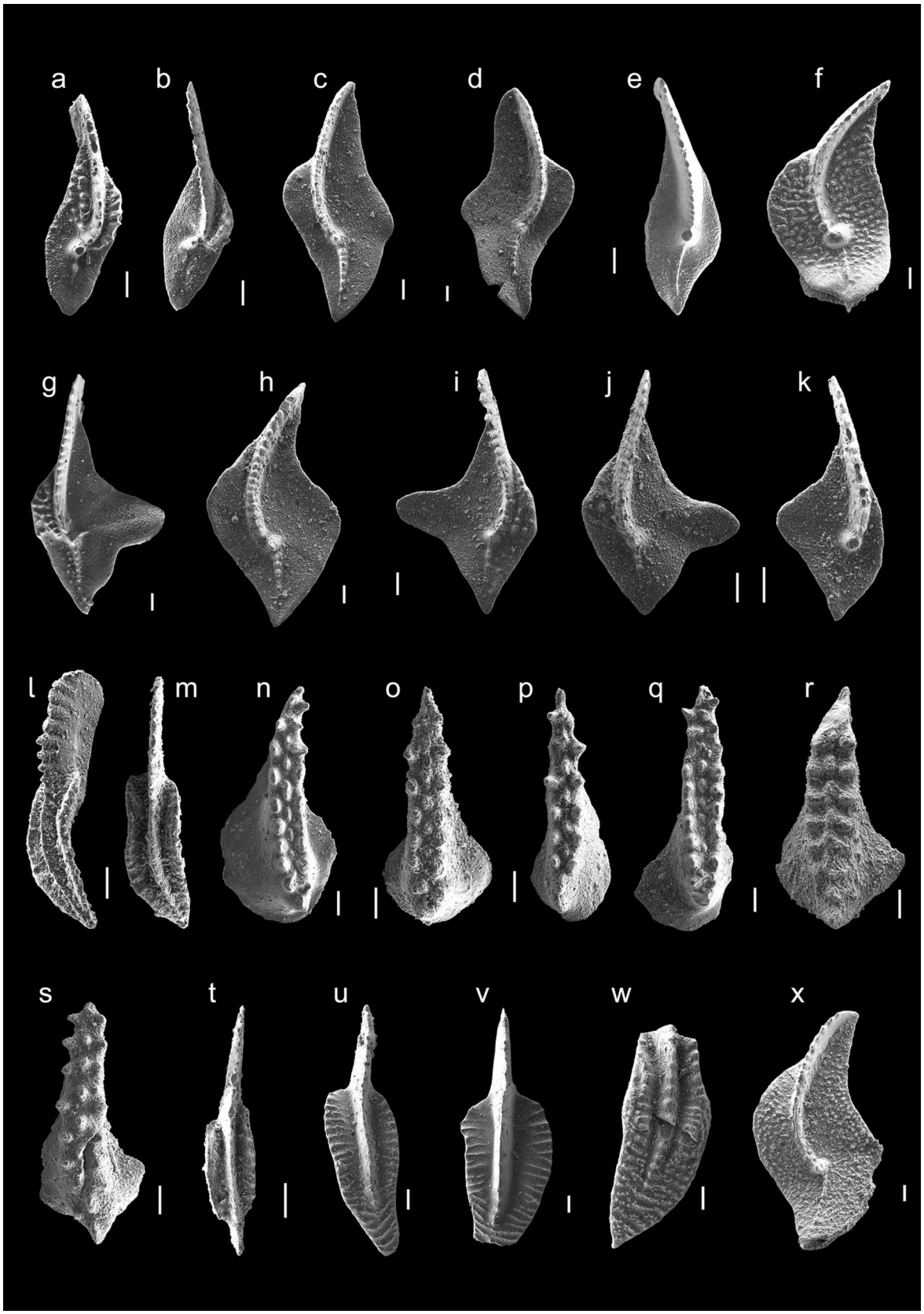
a
b
c
d
e
f
g
h
i
j
k
l
m
n
o
p
q
r
s
t
u
v
w
x

◂**Fig. 4** Conodonts from the Compte section (*Pa. gl. prima* to *Pa. gr. gracilis* zones). **a, b** *Palmatolepis termini* Sannemann, 1955a; **a** sample CP/98c; **b** sample CP/99d-2. **c** *Palmatolepis glabra prima* M1 Ziegler and Huddle, 1969; sample CP/98c. **d** *Palmatolepis tenuipunctata* Sannemann, 1955a; sample CP/99a. **e** *Palmatolepis minuta minuta* Branson and Mehl, 1934; sample CP/112e. **f** *Palmatolepis crepida* Sannemann, 1955a; sample CP/101a. **g** *Palmatolepis quadrantinodosalobata* Sannemann, 1955b; sample CP/98c. **h** *Palmatolepis regularis* Cooper, 1931; sample CP/99a. **i** *Palmatolepis subperlobata* Branson and Mehl, 1934; sample CP/99b. **j** *Palmatolepis lobicornis* Schülke, 1995; sample CP/99d-2. **k** *Palmatolepis minuta wolskae* Szulczewski, 1971; sample CP/99d-2. **l, m** *Polygnathus procerus* Sannemann, 1955b; sample CP/99a; **l** lateral view, **m** upper view. **n** *Icriodus alternatus mawsonae* Yazdi, 1999; sample CP/99d-2. **o** *Icriodus alternatus alternatus* Branson and Mehl, 1934; sample CP/99b. **p** *Icriodus alternatus alternatus* Branson and Mehl, 1934; sample CP/102b. **n** *Icriodus alternatus mawsonae* Yazdi, 1999; sample CP/99d-2. **r** *Icriodus tumulosus* Sanz-López, 1995; sample CP/104c. **s** *Icriodus cornutus* Sannemann, 1955b; sample CP/109b. **t** *Polygnathus brevilaminus* Branson and Mehl, 1934; sample CP/99a. **u, v** *Polygnathus semicostatus* Branson and Mehl, 1934; **u** sample CP/106; **v** sample CP/105b. **w** *Polygnathus bouckaerti* Dreesen and Dusar, 1974; sample CP/111a-1. **x** *Palmatolepis perlobata perlobata* Ulrich and Bassler, 1926; sample CP/104c. Scale bar = 100 µm

(sample CP/112a) in the Compte section. This taxon is restricted to the nominal zone. Concurrent with this first entry, *Palmatolepis per. helmsi* appears (sample CP/112a) and continues in the succeeding zone. Other taxa appearing at different levels within the lower part of the zone and continuing into the next zone include *Polygnathus subnormalis* (Fig. 5o) (sample CP/112b), *Polygnathus lauriformis* (Fig. 5m) (sample CP/112c) and *Palmatolepis gl. glabra* (Fig. 5e) (sample CP/112d). *Mehlina strigosa* (Figs. 5r–s) is recorded in samples CP/112c and CP/112f within this zone. *Polygnathus triphyllatus* (Fig. 5k) is recorded slightly higher (sample CP/112e). In the upper part of the zone, the successive records of *Palmatolepis quadrantinodosa inflexa* (Fig. 5x) (sample CP/112g, 1.35 m below the upper boundary of the zone) and *Palmatolepis stoppeli* (Fig. 5u) (sample CP/113c), 10 cm below the base of the next *Palmatolepis mg. marginifera* Zone) are noteworthy. Two other taxa from previous zones show their highest records within this zone: *Polygnathus semicostatus* (sample CP/112g) and *Polygnathus padovanii* (sample CP/113b). The following taxa, which appear in earlier zones, cross the zone: *Palmatolepis mint. minuta*, *Palmatolepis gl. prima*, *Polygnathus gb. glaber*, *Palmatolepis gl. pectinata*, *Polygnathus nod. nodocostatus*, *Polygnathus nod. ovatus*, *Palmatolepis per. schindewolfi, Palmatolepis rhomboidea*, *Palmatolepis gl. acuta,* and *Palmatolepis gl. lepta. Polygnathus com. communis* is recorded above and below the zone, but not within the *Pa. gr. gracilis* Zone. *Polygnathus subnormalis* ranges up near to the top of Bed 113 (sample CP/113c).

Palmatolepis marginifera marginifera Zone

The lower boundary of the *Palmatolepis mg. marginifera* Zone coincides nearly with the proposed base of the middle Famennian and is defined by the first occurrence of *Palmatolepis mg. marginifera* (Fig. 5aa) at the base of Bed 114 (sample CP/114a) (Fig. 3c). In the same sample, the lowest records of *Palmatolepis quad. inflexoidea* (Fig. 5y) and *Palmatolepis quad. quadrantinodosa* (Fig. 5z) are documented. The late morphotype of *Palmatolepis gl. lepta* (Fig. 5c) begins in sample CP/114b). Higher up (sample CP/117), *Palmatolepis per. sigmoidea* (Fig. 5v) (unique record) and. *Polygnathus gb. medius* (Fig. 5q) follow; the latter is recorded up to the last sampled bed (sample CP/120). The lowest (and unique) record of *Polygnathus longiusculus* (Fig. 5t) occurs in the upper part of this zone (sample CP/118b). In addition to these conodonts, many taxa with lowest occurrences in previous zones continue and have their highest records within this zone: *Palmatolepis mint. minuta* (highest record in sample CP/119), *Palmatolepis gl. prima* (sample CP/117), *Polygnathus gb. glaber* (sample CP/119), *Palmatolepis gl. pectinata* (sample CP/120), *Polygnathus nod. nodocostatus* (sample CP/116), *Polygnathus nod. ovatus* (sample CP/114b), *Palmatolepis per. schindewolfi* (CP/120), (sample CP/120), *Palmatolepis rhomboidea* (sample CP/120), *Palmatolepis gl. acuta* (sample CP/117), *Palmatolepis gl. lepta* late morphotype (sample CP/120), *Palmatolepis per. helmsi* (sample CP/119), *Poly-gnathus lauriformis* (sample CP/119), *Mehlina strigosa* (sample CP/114b), *Polygnathus triphyllatus* (sample CP/118a), *Palmatolepis quad. inflexa* (sample CP/120), *Palmatolepis stoppeli* (sample CP/119), and *Polygnathus com. communis* range up to the base of the zone (sample CP/114a).

This detailed zonation provides a robust framework for understanding the conodont biostratigraphy in the Compte section, offering critical insights into the lower to middle Famennian interval and contributing to the broader understanding of Famennian conodont distribution and evolution.

Discussion and comparison with previous data

Boersma (1973) investigated numerous sections and documented their conodont faunas in the Spanish Central Pyrenees, spanning from the Přídolí to the Lower Carboniferous. One of these sections was the Compte section, which includes the Villech Fm. and the Compte Fm. with its three members (A–C), corresponding to the Comabella, La Mena and Barousse Fms. respectively (Montesinos and Sanz-López 1999; Valenzuela-Ríos and Sanz-López 2002). The conodont record indicates that the age of these rocks ranges from Givetian to Tournaisian, with most of our study

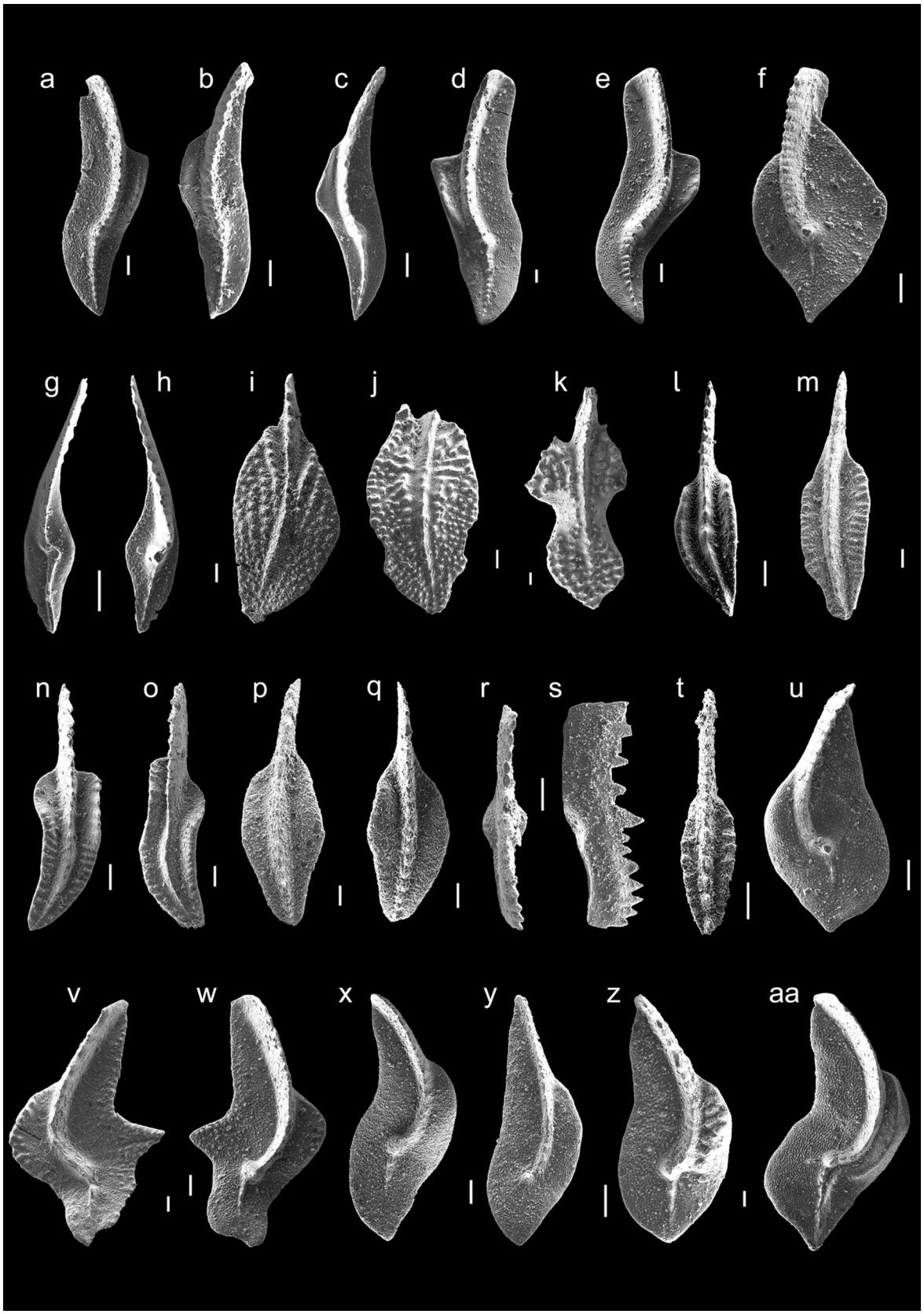
a
b
c
d
e
f
g
h
i
j
k
l
m
n
o
p
q
r
s
t
u
v
w
x
y
z
aa

◂**Fig. 5** Conodonts from the Compte section (*Pa. gl. pectinata* to *Pa. mg. marginifera* zones). **a** *Palmatolepis glabra pectinata* Ziegler, 1962b; sample CP/111b. **b** *Palmatolepis glabra lepta* early morphotype Ziegler and Huddle, 1969; sample CP/111c. **c** *Palmatolepis glabra lepta* late morphotype Ziegler and Huddle, 1969; sample CP/118b. **d** *Palmatolepis glabra acuta* Helms, 1963; sample CP/111b. **e** *Palmatolepis glabra glabra* Ulrich and Bassler, 1926; sample CP/112d. **f** *Palmatolepis rhomboidea* Sannemann, 1955a; sample CP/110. **g, h** *Palmatolepis gracilis gracilis* Branson and Mehl, 1934; sample CP/112a; **g** lower view, **h** upper view. **i** *Polygnathus nodocostatus nodocostatus* Branson and Mehl, 1934; sample CP/112a. **j** *Polygnathus nodocostatus ovatus* Helms, 1961; sample CP/105a. **k** *Polygnathus triphyllatus* Helms, 1961; sample CP/112e. **l** *Polygnathus communis communis* Branson and Mehl, 1934; sample CP/107. **m** *Polygnathus lauriformis* Dreesen and Dusar, 1974; sample CP/113a. **n** *Polygnathus padovanii* Perri and Spalletta, 1990; sample CP/112e. **o** *Polygnathus subnormalis* Vorontsova and Kuzmin, 1984; sample CP/112b. **p** *Polygnathus glaber glaber* Ulrich and Bassler, 1926; sample CP/112b. **q** *Polygnathus glaber medius* Helms and Wolska, 1967; sample CP/119. **r, s** *Mehlina strigosa* Branson and Mehl, 1934; sample CP/114a; **r** upper view, **s** lateral view. **t** *Polygnathus longiusculus* Çapkınoğlu, 1997; sample CP/118b. **u** *Palmatolepis stoppeli* Sandberg and Ziegler, 1973; sample CP/113c. **v** *Palmatolepis perlobata sigmoidea* Ziegler, 1962a. **w** *Palmatolepis perlobata schindewolfi* Müller, 1956; sample CP/119. **x** *Palmatolepis quadrantinodosa inflexa* Müller, 1956, **y** *Palmatolepis quadrantinodosa inflexoidea* Ziegler, 1962a; sample CP/114a. **z** *Palmatolepis quadrantinodosa quadrantinodosa* Branson and Mehl, 1934; sample CP/114a. **aa** *Palmatolepis marginifera marginifera* Helms, 1959. Scale bar = 100 µm

focusing on La Mena Fm. Boersma (1973, fig. 6) assigned his beds 321–329 to the B-Member (i.e. La Mena Fm.). We have been able to recognise Boersma (1973) sample levels and establish a correlation with his studies where results differ.

The sample in Boersma's Bed 321, which corresponds to our Bed 106, yielded a Frasnian conodont fauna (see Boersma 1973, table 1); as a result, Boersma assigned the base of La Mena Fm. to the *gigas* Zone (equivalent to the current FZ13 Zone), which do not align with our analysis. Recently, the Frasnian–Famennian boundary was identified within the upper part of Comabella Fm. in Bed 92 (Silvério et al. 2021). The overlaying strata, Beds 93–97, were assigned to the Famennian *Pa. mint. minuta–Pa. crepida* zones. Our Bed 106 is assigned to the upper part of the *Palmatolepis glabra pectinata* Zone, which is clearly Famennian.

The next sample (322) was aligned with the base of the Famennian, the *Palmatolepis triangularis* Zone, corresponding to the Boersma's time leading zonation (Ziegler 1962a). This sample would correspond to our Beds 107–109, and our records indicate these beds belong to the *Palmatolepis rhomboidea* Zone.

Boersma's sample 323, located in the lower half of our Bed 112, yielded the lowest record of *Palmatolepis crepida*, the index of the *Palmatolepis crepida* Zone; consequently, the base of this zone was placed at this level. However, our lowest record of *Palmatolepis crepida* occurs in Bed 98; the taxon is even recorded earlier, in the basal 8 cm of Bed 94 (sample CP/94a of Silvério et al. 2021). Moreover, the conodonts from the lower part of our Bed 112 identify the *Palmatolepis gr. gracilis* Zone.

Boersma documented the lowest record of *Palmatolepis rhomboidea* in his Bed 326; thus, he places the base of the *Palmatolepis rhomboidea* Zone at this level. This bed can be aligned with our Bed 114. In contrast, our lowest record of this index taxon is recorded in Bed 107, almost 5 m lower. Bed 114 provided conodonts of the *Palmatolepis mg. marginifera* Zone, including its index taxon.

Finally, Boersma identified the beginning of the *Palmatolepis quadrantinodosa* Zone (equivalent to the current *Palmatolepis mg. marginifera* Zone) in his Bed 329, which would be situated near the top of our Bed 115. Our records, however, locate the base of the *Palmatolepis mg. marginifera* Zone, slightly below, close to the base of Bed 114.

In brief, Boersma bracketed the La Mena Fm. in the section Compte between the uppermost Frasnian and lower–middle Famennian zones. However, the results of our research suggest that La Mena Fm. is much younger than his interpretation. The *Palmatolepis termini, Palmatolepis gl. prima* and *Palmatolepis gl. pectinata* zones are identified in Beds 98–106, belonging to the highest Comabella Fm. and the base of La Mena Fm. (Bed 106). Above follow the *Palmatolepis rhomboidea* and *Palmatolepis gr. gracilis* zones (Beds 107–113), which are exclusively restricted to the La Mena Fm. Finally, the *Palmatolepis mg. marginifera* Zone (Beds 114–120) spans from the highest La Mena Fm. through the lower part of the Barousse Fm.

In a partial revision of the unpublished material of Silvério et al. (2021), we have identified *Palmatolepis termini* in Bed 96, which was formerly assigned to the *Palmatolepis crepida* Zone; this information is coherent with our analysis and, consequently, the nominal zone starts below the studied part of the Compte section reported here.

Most conodont ranges documented in the Compte section are shorter than their global known ranges. This is particularly observed in beds assigned to the *Palmatolepis termini*, *Palmatolepis gl. prima*, *Palmatolepis glabra pectinata*, and *Palmatolepis rhomboidea* zones. Regarding the *Palmatolepis termini* Zone, the lowest records of *Palmatolepis mint. minuta* and *Palmatolepis quadrantinodosalobata* in the Compte section are delayed, as the former is the index of the homonymous zone and the morphotype 2 of the latter is recorded at the base of the underlying *Palmatolepis crepida* Zone (Spalletta et al. 2017).

Concerning the *Palmatolepis gl. prima* Zone, the highest record of *Palmatolepis termini* occurs in the lower half of the zone, while elsewhere it can reach the uppermost levels of this zone (Spalletta et al. 2017). The local extinction of *Icriodus alt. mawsonae* aligns with the global range of this taxon. Other local highest ranges differ, as they have a

higher range elsewhere*: Palmatolepis lobicornis* reaches the lower half of the *Palmatolepis rhomboidea* Zone; the highest range of *Palmatolepis tenuipunctata* is known to reach the overlying *Palmatolepis gl. pectinata* Zone, and *Palmatolepis quadrantinodosalobata* (morphotype 2) and *Palmatolepis crepida* are recorded up to the *Palmatolepis rhomboidea* Zone. Similarly, the lowest records of the following taxa, which have their entries in the *Palmatolepis glabra prima* Zone, in the Compte section, are delayed relative to their worldwide occurrences: *Palmatolepis subperlobata* enters in the nominal zone at the base of the Famennian; *Palmatolepis regularis* and *Polygnathus procerus* start within the *Palmatolepis mint. minuta* Zone; *Palmatolepis mint. loba* enters in the *Palmatolepis crepida* Zone, and both *Polygnathus gb. glaber* and *Polygnathus semicostatus* range from the *termini* Zone. However, in a recent revision of the unpublished material of Silvério et al. (2021) *Palmatolepis subperlobata* and in the upper part of Bed 92 (*Palmatolepis del. platys* Zone), and *Palmatolepis regularis* in Bed 94 (*Palmatolepis crepida* Zone).

In the *Palmatolepis glabra pectinata* Zone, the lowest records, coinciding with the base of the zone, of *Palmatolepis per. perlobata* and *Polygnathus padovanii* differ from those of other regions. The former is already recorded from the *Palmatolepis mint. minuta* Zone, and the latter has its lowest records within the upper half of the zone (Spalletta et al. 2017). Slightly higher, *Polygnathus nod. nodocostatus* and *Palmatolepis perlobata schindewolfi* enter. *Polygnathus com. communis* enters in sample CP/106; however, in the recent revision of unpublished material of Silvério (2021), this taxon enters in Bed 94 (upper part of *Palmatolepis crepida* Zone). The two former taxa occur in many places already from the *Palmatolepis crepida* Zone, and the latter enters within the preceding *Palmatolepis glabra prima* Zone. The highest local record of *Palmatolepis mint. wolskae* is lower than common records, which show its range up to the *Palmatolepis rhomboidea* Zone. Sanz-López (1995) documented the range of *Icriodus tumulosus* from the *Palmatolepis gl. pectinata* to the *Palmatolepis rhomboidea* zones in the Cadí Nape; however, in the Compte section, this taxon is only recorded at the base of the *Palmatolepis pectinata* Zone. The range of *Polygnathus padovanii* is under discussion: Perri and Spalletta (1990) initially indicated the range from the *Palmatolepis mg. utahensis* to the *Palmatolepis r. trachytera* zones in the Carnic Alps. Later, Corradini (2003) suggested a longer record in this area. However, the lower range of *Polygnathus padovanii* is lower in Iranian regions than previously assigned (Perri and Spalletta 1990): from the *Palmatolepis gl. pectinata* Zone (Bahrami et al. 2022) or from the *Palmatolepis rhomboidea* Zone (Sattari et al. 2021). The range of *Polygnathus padovanii* in the Compte section extends from the base of the *Palmatolepis gl. pectinata* Zone to the upper part of the *Palmatolepis gr. gracilis* Zone; it could range higher, but we have not sampled higher levels in this study.

In the Compte section, all entries within the *Palmatolepis rhomboidea* Zone, are delayed. *Palmatolepis* cf. *klapperi* and the early morphotype *Palmatolepis glabra lepta* are known from the *Palmatolepis gl. prima* Zone in other parts. The global range of *Icriodus cornutus* starts from the *Palmatolepis delicatula platys* Zone, and in the studied section is recorded within the middle part of *the Palmatolepis rhomboidea* Zone sample (CP/109/b). *Icriodus alt. alternatus* is recorded 1.3 m above the base of the *Palmatolepis rhomboidea* Zone (sample CP/111a-1) in the Compte section, which is higher than the previously assigned range that extends up to the top of *Palmatolepis gl. pectinata* Zone (Bultynck 2003; Spalletta et al. 2017).

The range of *Palmatolepis gr. gracilis* is restricted to the nominal zone in the Compte section, while globally it extends to the *Bispathodus ultimus* Zone. For the *Palmatolepis gr. gracilis* Zone, there are critical conodonts such as *Polygnathus triphyllatus* and *Palmatolepis stoppeli* that have worldwide range and are also found in the Compte section. *Palmatolepis quad. inflexa* also appears globally in this zone. The first occurrences of three taxa are delayed in the Compte section: both *Polygnathus lauriformis* and *Mehlina strigosa*, which range from the *Palmatolepis termini* Zone elsewhere, and *Palmatolepis per. helmsi*, which is known from the *Palmatolepis rhomboidea* Zone. Additionally, the index taxon, which is restricted in the Compte section to the lower part of the zone, and *Polygnathus semicostatus* and *Polygnathus padovanii,* have their highest ranges much lower in the Compte section than globally (compare Spalletta et al. 2017).

The base of the *Palmatolepis mg. marginifera* Zone is defined by the entry of its index taxon. Additionally, *Palmatolepis quad. inflexoidea* starts at the base of *Palmatolepis mg. marginifera* Zone (Spalletta et al. 2017), and *Palmatolepis quad. quadrantinodosa* is exclusively recorded in this zone (Spalletta et al. 2017). The disappearance of *Polygnathus triphyllatus* and *Palmatolepis stoppeli* align with the worldwide extinctions within this zone. At 1.2 m above the base (sample CP/117), *Palmatolepis per. sigmoidea* is recorded, in agreement with its global entry (Spalletta et al. 2017). The global entry of *Polygnathus gb. medius* coincides with the base of the *Palmatolepis mg. marginifera* Zone (Ji and Ziegler 1993), but in the Compte section, its entry is delayed, occurring 1.2 m above the base of the zone (sample CP/117). In sample CP/118b, *Polygnathus longiusculus* appears, a taxon exclusive of this zone (Çapkınoğlu 1993). According to Sandberg and Ziegler (1973) and Hartenfels (2011), the late morphotype of *Palmatolepis gl. lepta* (Fig. 5c) appears at the base of the *mg. marginifera* Zone. However, in the Compte section, this taxon appears 40 cm above the base of the zone (sample CP/114b). The range of the early morphotype of *Palmatolepis*

gl. lepta (Fig. 5b) extends from the *Palmatolepis gl. prima* Zone to the upper part of the *Palmatolepis gr. gracilis* Zone (Sandberg and Ziegler 1973; Hartenfels 2011). In South China, it is recorded within the *Palmatolepis mg. marginifera* Zone to *Palmatolepis mg. utahensis* Zone (Huang et al. 2024b), and in the Compte section, it is documented 40 cm above the base of the *Palmatolepis mg. marginifera* Zone (sample CP/114b).

Brief comments on lower and middle Famennian Global Events and their expressions in the Compte section

Following the mass extinction associated to the Kellwasser Events around the Frasnian–Famennian boundary, several minor Global Events were identified during the lower to middle Famennian. The first event, known as the Nehden Event, is associated with an eustatic rise in sea level during the lower Famennian (Walliser 1996; House 2002; Zhang et al. 2019), contrasting with interpretations of a regressive phase (Schülke 2003; Schülke and Popp 2005). The Nehden Event is characterised by a gradual biotic recovery of various taxa, including conodonts, ammonoids and brachiopods (House 2002; Becker et al. 2020; Huang et al. 2024b). It is recognised across Euramerica, Africa and Australia by deposits of ammonitic black shales (Becker 1993; Becker and House 1997; Schülke and Popp 2005; Becker et al. 2016). However, uncertainties remain regarding the evolution rates, timing, and magnitude of its impact, with its duration generally spanning from the *Palmatolepis termini* to the *Palmatolepis gl. pectinata* zones (Becker et al. 2020). In the Compte section, the Nehden Event is not discernible by lithological changes; however, the increase of *Palmatolepis* abundance during the *Palmatolepis termini–Palmatolepis gl. prima* zones may represent a biotic expression of Nehden event in this Pyrenean section.

The Condroz Event, comprises two regressive pulses during the lower to middle Famennian (Walliser 1996; Becker and House 1997; Schülke and Popp 2005). The first pulse is marked by a significant sea–level fall during the *Palmatolepis rhomboidea* Zone. The second pulse occurred during the transition from the *Palmatolepis gr. gracilis* to *Palmatolepis mg. marginifera* zones. In the Compte section, the change in conodont faunas observed within the *Palmatolepis rhomboidea* Zone may be a consequence of the first Condroz pulse; however, the second pulse is not clear to be identified.

Conclusions and summary

An extensive conodont sampling in the Compte section has yielded a diverse recovery of 47 conodont taxa belonging to four genera (*Palmatolepis, Polygnathus, Icriodus* and *Mehlina*). This conodont assemblage lead to a detailed biostratigraphy, identifying six consecutive conodont zones spanning the lower to middle Famennian and precisely locating the base of the middle Famennian in the Compte section. These zones include the *Palmatolepis termini* Zone, *Pa. glabra prima* Zone, *Pa. glabra pectinata* Zone, *Pa. rhomboidea* Zone, *Pa. gracilis gracilis* Zone and *Pa. mg. marginifera* Zone, encompassing the upper part of the Comabella Fm., La Mena Fm. and the lower strata of the Barousse Fm.

The lowest biostratigraphical unit identified is the *Palmatolepis termini* Zone, comprising the lowermost 60 cm of the analysed section (Bed 98, samples a–b), where the entry of several lower Famennian taxa such as *Palmatolepis tenuipunctata*, *Icriodus alt. alternatus*, *Palmatolepis quadrantinodosalobata* and *Palmatolepis crepida* is observed. The *Palmatolepis gl. prima* Zone begins with the entry of the *Palmatolepis gl. prima* morphotype 1 in the upper part of Bed 98, within this zone numerous conodont taxa have their lowest local ranges. The *Palmatolepis gl. pectinata* Zone is marked by the entry of *Palmatolepis gl. pectinata* in the uppermost 10 cm of Bed 104, accompanied by changes in conodont fauna dominated by *Palmatolepis glabra* and *Polygnathus nodocostatus*-stocks and *Polygnathus semicostatus*.

The *Palmatolepis rhomboidea* Zone starts in Bed 107, 19 cm above the base of La Mena Fm., with the entry of its index taxon. The *Palmatolepis gr. gracilis* Zone starts in Bed 112 with the entry of *Palmatolepis gr. gracilis*; through into the *Palmatolepis mg. marginifera* Zone, where taxa such as *Polygnathus triphyllatus*, *Palmatolepis quad. inflexa* and *Palmatolepis stoppeli* are found in the upper half. The *Palmatolepis mg. marginifera* Zone begins at the base of Bed 114 with the entry of *Palmatolepis mg. marginifera*, alongside *Pa. quad. inflexoidea* and *Pa. quad. quadrantinodosa*. The delayed entry of *Polygnathus gb. medius* is noted 1.2 m above the base of the *Palmatolepis mg. marginifera* Zone, while both morphotypes of *Palmatolepis gl. lepta* appear in sample CP/114b, with the early morphotype documented slightly above its global records.

The La Mena Fm. in the Compte section is exclusively Famennian, extending from the upper *Palmatolepis glabra pectinata* Zone to the *Palmatolepis mg. marginifera* Zone, spanning the lower–middle Famennian transition located at the base of the *Palmatolepis mg. marginifera* Zone.

Comparison with Boersma's conodont zonation shows discrepancies primarily at the top of the Comabella and La Mena Fm., necessitating modifications. The base of the La Mena Fm. (Bed 106) is reinterpreted as located in the uppermost part of the Famennian *Palmatolepis gl. pectinata* Zone, rather than in the Frasnian (*gigas* Zone= FZ13) as assigned by Boersma. The lower Famennian *Palmatolepis triangularis* to *Palmatolepis crepida* zones are situated within the Comabella Fm. in the Compte section, in contrast with Boersma's interpretation The beginning of the *Palmatolepis*

rhomboidea Zone is placed significantly lower than suggested by Boersma, although the base of the *Palmatolepis mg. marginifera* Zone is only slightly lower than Boersma's interpretation,

Furthermore, the succession of conodont associations in the Compte section provides initial insights into the effects of the Nehden and Condroz events in the Pyrenean sections. However, a comprehensive analysis integrating litho-biofacies with geochemichal and geophysical data will be essential for a thorough understanding.

Finally, a biostratigraphic reinterpretation of the upper beds (96 and 97) of the Compte section, based on the revision of the samples of Silverio et al. (2021), confirms their assignment to the *Palmatolepis termini* Zone rather than the *Palmatolepis crepida* Zone as these authors suggested.

Acknowledgements We dedicate this work to our long-time and lovely friend Peter Königshof on the occasion of his retirement from the Senckenberg Research Institute and Natural History Museum Frankfurt. We are very grateful for his camaraderie, his time and teachings, all the good times we had together and for his continuous inspiration and support of international cooperation and, specially, of young researchers. We are very thankful to Dr. J. Over and Dr. C. Spalletta for their helpful comments in the editorial reviews.

This work represents a contribution to the Project IGCP-652 of UNESCO and, in addition, it conforms a contribution of the research groups GIUV2017-395, GEO-TRANSFER E32 17R and PERIGONDWANA UCM 910231. We are thankful to the Microscopy section of the Support Research Center, University of Valencia. We also thank the facilities provided by the UNESCO Global Geopark Orígens to carry out our work.

Funding Open Access funding provided thanks to the CRUE-CSIC agreement with Springer Nature. J. C-L is supported by Maria Zambrano Grant (MIU Next Generation EU, ZA21-005) and José Castillejo Fellowship (MICCIN-MIU, CAS22/00148). H. B-L is supported by Sociedad Española de Paleontología. This report is a contribution to UCM DEVOCLIMEVENTS Research Grant (PR12/24-31569).

Data availability All data and materials that provides the research results are available within this article and extended in Barrera-Lahoz et al. (2024). The fossil conodont remains, which provide the article data, are housed in the "Department of Botany and Geology" at the University of Valencia, Burjasot, Spain.

Compliance with ethical standards

Conflict of interest The authors declare that they have no conflict of interest.

References

Bahrami, A., Königshof, P., Hartkopf-Fröder, C., & Kaiser, S. I. (2022). Late Devonian–Mississippian conodont biostratigraphy of the Chelcheli section, NE Shahrud (Eastern Alborz, North Iran). *Paläontologische Zeitschrift*, *96*(3), 449–469. https://doi.org/10.1007/s12542-021-00575-6

Barnolas, A., & Pujalte, V. (2004). La Cordillera Pirenaica. Definición, límites y división. In J. A. Vera (Ed.), *Geología de España* (pp. 233–240). Madrid: SGE-IGME.

Barrera-Lahoz, H., Valenzuela-Ríos, J. I., & Liao, J.-C. (2024). Famennian conodont assemblage in the Compte section (Upper Devonian, Central Pyrenees) and its comparison with Eurasian sequences. *Spanish Journal of Palaeontology*, *39*(1), 33–70. https://doi.org/10.7203/sjp.28695

Becker, R. T., (1993). Stratigraphische Gliederung und Ammonoideen-Faunen im Nehdenium (Oberdevon II) von Europa und Nord-Afrika. *Courier Forschungsinstitut Senckenberg*, *155*, 1–405.

Becker, R. T., & House, M. R. (1997). Sea-level changes in the Upper Devonian of the Canning Basin, western Australia. *Courier Forschungsinstitut Senckenberg* , *199*, 129–146.

Becker, R. T., Gradstein, F. M., & Hammer, O. (2012). The Devonian Period. In F. M. Gradstein, J. G. Ogg, M. D. Schmitz, & G. M. Ogg (Eds.), *The Geologic Time Scale* (2nd vol. pp. 559–601). Amsterdam: Elsevier.

Becker, R.T., Hartenfels, S., Helling, S., Schreiber, G., (2016). The "Nehden Goniatite Shale" (lower Famennian, Brilon Reef complex, NE Rhenish Massif). *Münstersche Forschungen zur Geologie und Paläontologie*, *108*, 179–195.

Becker, R.T., Marshall, J.E.A., Da Silva, A.C., Agterberg, F.P., Gradstein, F.M., & Ogg, J.G., (2020). The Devonian Period. In F. P. Agterberg, F. M. Gradstein, J. G. Ogg (Eds.), *The Geologic Time Scale* (2nd vol. pp. 733–810). Elsevier. https://doi.org/10.1016/B978-0-12-824360-2.00022-X

Boersma, K. T. (1973). Devonian and Lower Carboniferous conodont biostratigraphy, Spanish Central Pyrenees. *Leidse Geologische Mededelingen*, *49*(2), 303–377.

Branson, E. B., & Mehl, M. G. (1934). Conodonts from the Grassy Creek shale of Missouri. *Missouri University Studies*, *8*, 171–259.

Bultynck, P. (2003). Devonian Icriodontidae: biostratigraphy, classification and remarks on paleoecology and dispersal. *Revista Española de Micropaleontología*, *35*(3), 295–314.

Çapkınoğlu, Ş. (1997). Conodont fauna and biostratigraphy of the Famennian of Büyükada, Istanbul, Northwestern Turkey. *Bollettino della Società Paleontologica Italiana*, *35*(2), 165–186.

Cooper, C. L. (1931). New conodonts from the Woodford Formation of Oklahoma. *Journal of Paleontology*, *5*(3), 230–243.

Corradini, C. (2003). Late Devonian (Famennian) conodonts from the Corona Mizziu Sections near Villasalto (Sardinia, Italy). *Palaeontographia Italica*, *89*, 65–116.

Dreesen, R., & Dusar, M. (1974). Refinement of conodont-biozonation in the Famenne area. In J. P. Bouckaert, & M. Street (Eds.), *International Symposium on Belgian Micropaleontological Limits from Emsian to Viséan* (pp. 1–38.). Namur: Geological Survey of Belgium, 13.

Girard, C., Cornee, J. J., Corradini, C., Fravalo, A., & Feist, R. (2014). Palaeoenvironmental changes at Col des Tribes (Montagne Noire, France), a reference section for the Famennian of north

Gondwana-related areas. *Geological Magazine*, *151*(5), 864–884. https://doi.org/10.1017/S0016756813000927

Gouwy, S., Liao, J.-C., & Valenzuela-Ríos, J. I. (2013). Eifelian (Middle Devonian) to Lower Frasnian (Upper Devonian) conodont biostratigraphy in the Villech section (Spanish Central Pyrenees). *Bulletin of Geosciences*, *88*(2), 315–338. https://doi.org/10.3140/bull.geosci.1341

Hartenfels, S. (2011). *Die globalen Annulata-Events und die Dasberg-Krise (Famennium, Oberdevon) in Europa und Nord-Afrika: hochauflösende Conodonten-Stratigraphie, Karbonat-Mikrofazies, Paläoökologie und Paläodiversität*. PhD Thesis, Münster: Universität Münster.

Hartevelt, J. J. A. (1970). Geology of the upper Segre and Valira valleys, central Pyrenees, Andorra/Spain. *Leidse Geologische Mededelingen*, *45*(1), 167–236.

Helms, J. (1959). Conodonten aus dem Saalfelder Oberdevon (Thuringen). *Geologie*, *8*, 634–677.

Helms, J. (1961). Die "nodocostata-Gruppe" der Gattung *Polygnathus*. *Geologie*, *10*(6), 674–711.

Helms, J. (1963). Zur "Phylogenese" und Taxonomie von *Palmatolepis* (Conodontida, Oberdevon). *Geologie*, *12*, 449–485.

Helms, J., & Wolska, Z. (1967). New Upper Devonian conodonts from Poland and Germany. *Acta Palaeontologica Polonica*, *12*(2), 227–238.

House, M. R. (2002). Strength, timing, setting and cause of mid-Palaeozoic extinctions. *Palaeogeography, Palaeoclimatology, Palaeoecology*, *181*(1–3), 5–25. https://doi.org/10.1016/S0031-0182(01)00471-0

Huang, Y. Z., Qi, Y. P., Wang, Q. L., Yao, L., & Chen, J. T. (2024a). Latest Devonian–Early Mississippian conodont biostratigraphy in the Naqing section, Guizhou, South China. *Palaeoworld*, *33*(2), 307–327. https://doi.org/10.1016/j.palwor.2023.02.004

Huang, C., Song, H., Zhai, M., Pu, T., & Han, M. (2024b). Timing and pattern of the Devonian Nehden event: Implication for the biotic recovery following the F–F extinction event. *Palaeogeography, Palaeoclimatology, Palaeoecology*, *648*, 112276. https://doi.org/10.1016/j.palaeo.2024.112276

Institut Cartogràfic i Geològic de Catalunya (2023, September 20th). *Mapa Geològic de Catalunya 1:25000*. https://betaportal.icgc.cat/visor/client_utfgrid_geo.html

Ji, Q., & Ziegler, W. (1993). The Lali section: an excellent reference section for Late Devonian in south China. *Courier Forschungsinstitut Senckenberg* , *157*, 1–183.

Klapper, G. (2007). Conodont taxonomy and the recognition of the Frasnian/Famennian (Upper Devonian) stage boundary. *Stratigraphy*, *4*(1), 67–76.

Klapper, G., Uyeno, T. T., Armstrong, D. K., & Telford, P. G. (2004). Conodonts of the Williams Island and Long Rapids formations (Upper Devonian, Frasnian–Famennian) of the Onakawana B Drillhole, Moose River Basin, northern Ontario, with a revision of Lower Famennian species. *Journal of Paleontology*, *78*(2), 371–387. https://doi.org/10.1666/0022-3360(2004)078<0371:COTWIA>2.0.CO;2

Liao, J.-C., & Valenzuela-Ríos, J. I. (2008). Givetian and early Frasnian conodonts from the Compte section (Middle–Upper Devonian, Spanish Central Pyrenees). *Geological Quaterly*, *52*(1), 1–18.

Liao, J.-C., & Valenzuela-Ríos, J. I. (2013). The Middle and Upper Devonian conodont sequence from La Guardia D'Àres Sections (Spanish Central Pyrenees). *Bulletin of Geosciences*, *88*(2), 339–368. https://doi.org/10.3140/bull.geosci.1348

Liao, J.-C., & Valenzuela-Ríos, J. I. (2017). *Givetian to Famennian conodonts (Middle–Upper Devonian) at CP section* (pp. 99–105). Valencia: International Conodont Symposium 4. Progress on Conodont investigation.

Marshall, J. E. A. (2005). Minutes of the SDS Business Meeting, Rabat, 1st of March 2004. *SDS Newsletter*, *21*, 3–8.

Martínez-Pérez, C., Valenzuela-Ríos, J. I., Navas-Parejo, P., Liao, J. C., & Botella, H. (2011). Emsian (Lower Devonian) Polygnathids (Conodont) succession in the Spanish Central Pyrenees. *Journal of Iberian Geology*, *37*(1), 45–64. https://doi.org/10.5209/revJIGE.2011.v37.n1.4

Mey, P. H. W. (1967a). The geology of the upper Ribagorzana and Baliera valleys, Central Pyrenees, Spain. *Leidse Geologische Mededelingen*, *41*, 153–220.

Mey, P. H. W. (1967b). *Evolution of the Pyrenean Basins during the Late Paleozoic* (pp. 1157–1166). Calgary: International Symposium on the Devonian System.

Montesinos, J. R., & López, J. S. (1999). Ammonoideos del Devónico Inferior y Medio en el Pirineo Oriental y Central. Antecedentes históricos y nuevos hallazgos. *Spanish Journal of Palaeontology*, *14*(3), 97–108. https://doi.org/10.7203/sjp.23952

Müller, K. J. (1956). Die Gattung *Palmatolepis*. Zur Kenntnis der Conodonten-Fauna des europaischen Devons, 1. *Abhandlungen der Senckenbergischen Naturforschenden Gesellschaft*, *494*, 1–70.

Perri, M. C., & Spalletta, C. (1990). Famennian conodonts from climenid pelagic limestone, Carnic Alps, Italy. *Palaeontographia Italica*, *77*, 55–83.

Sánchez de Posada, L. C., Sanz-López, J., & Gozalo, R. (2008). Ostracod and conodont faunal changes across the Frasnian–Famennian (Devonian) boundary at Els Castells, Spanish central Pyrenees. *Revue de Micropaléontologie*, *51*(3), 205–219. https://doi.org/10.1016/j.revmic.2007.06.001

Sandberg, C. A., & Ziegler, W. (1973). Refinement of standard Upper Devonian conodont zonation based on sections in Nevada and West Germany. *Geologica et Palaeontologica*, *7*, 97–122.

Sannemann, D. (1955a). Beitrag zur Untergliederung des Oberdevons nach Conodonten. *Neues Jahrbuch für Geologie und Paläontologie, Abhandlungen*, *100*(3), 324–331.

Sannemann, D. (1955b). Oberdevonische Cconodonten (to II). *Senckenbergiana lethaea, 36, 123–156.*

Sanz-López, J. (1995). *Estratigrafía y bioestratigrafía (conodontos) del Silúrico superior–Carbonífero inferior del Pirineo oriental y central*. PhD Thesis. Barcelona: Universitat de Barcelona.

Sattari, E., Bahrami, A., Königshof, P., & Vaziri-Moghaddam, H. (2021). Late Devonian (Famennian) to Carboniferous (Mississippian–Pennsylvanian) conodonts from the Anarak section, Central Iran. *Palaeobiodiversity and Palaeoenvironments*, *101*(3), 781–802. https://doi.org/10.1007/s12549-020-00462-z

Schülke, I. (1995). Evolutive Prozesse bei *Palmatolepis* in der frühen Famenne-Srufe (Conodonta, Ober–Devon). *Göttinger Arbeiten zur Geologie und Paläontologie*, *67*, 1–108.

Schülke, I (2003) Famennian conodont biodiversity cycles. *Courier Forschungsinstitut Senckenberg*, *242*, 225–237.

Schülke, I., & Popp, A. (2005). Microfacies development, sea-level change, and conodont stratigraphy of Famennian mid-to deep platform deposits of the Beringhauser Tunnel section (Rheinisches Schiefergebirge, Germany). *Facies*, *50*, 647–664. https://doi.org/10.1007/s10347-004-0041-6

Schülke, I., Korn, D., Popp, A. & Ziegler, W. (2003). Potential reference section for the Early/Middle Famennian boundary at the Beringhauser Tunnel (Rheinisches Schiefergebirge, NW Germany). *SDS Newsletter*, *19*, 36–46.

Silvério, G. G., Valenzuela-Ríos, J. I., & Liao, J.-C. (2021). Upper Frasnian and Lower Famennian (Upper Devonian) conodonts of the Compte section (Spanish Central Pyrenees). *Spanish Journal of Palaeontology*, *36*(2), 205–220. https://doi.org/10.7203/sjp.36.2.21950

Slavík, L., Valenzuela-Ríos, J. I., Hladil, J., Chadimová, L., Liao, J. C., Hušková, A., Calvo, H. & Hrstka, T. (2016). Warming or cooling in the Pragian? Sedimentary record and petrophysical logs across the Lochkovian–Pragian boundary in the Spanish Central

Pyrenees. *Palaeogeography, Palaeoclimatology, Palaeoecology*, *449*, 300–320. https://doi.org/10.1016/j.palaeo.2016.02.018

Spalletta, C., Perri, M. C., Over, D. J., & Corradini, C. (2017). Famennian (Upper Devonian) conodont zonation: revised global standard. *Bulletin of Geosciences*, *92*(1), 31–57. https://doi.org/10.3140/bull.geosci.1623

Szulczewski, M. (1971). Upper Devonian conodonts, stratigraphy and facial development in the Holy Cross Mts. *Acta Geologica Polonica*, *21*(1), 1–130.

Ulrich, E. O., & Bassler, R. S. (1926). A classification of the tooth-like fossils, conodonts, with descriptions of American Devonian and Mississipian species. *Proceedings of the United States National Museum*, *68*, 1–63. https://doi.org/10.5479/si.00963801.68-2613.1

Valenzuela-Ríos, J. I., & Liao, J.-C. (2006). Annotations to Devonian Correlation Table, R 357–360 di-ds 06: Spanish Central Pyrenees, southern part. *Senckenbergiana lethaea*, *86*, 105–107. https://doi.org/10.1007/BF03043640

Valenzuela-Ríos, J. I., & Liao, J. C. (2012). Color/facies changes and Global Events, a hoax? A case study from the Lochkovian (Lower Devonian) in the Spanish Central Pyrenees. *Palaeogeography, Palaeoclimatology, Palaeoecology*, *367*, 219–230. https://doi.org/10.1016/j.palaeo.2011.09.007

Valenzuela-Ríos, J. I., & Liao, J. C. (2024). Biodiversity and evolutionary phases of Lochkovian (Lower Devonian) conodonts in the Pyrenees: A comparative study. *Marine Micropaleontology*, *187*, 102326. https://doi.org/10.1016/j.marmicro.2023.102326

Valenzuela-Ríos, J.I. & Sanz-López, J. (2002). Pyrenees. In W. Gibbons, & T. Moreno (Eds.), *The Geology of Spain* (pp. 86–89). Geological Society of London.

Valenzuela-Ríos, J. I., Slavík, L., Liao, J. C., Calvo, H., Hušková, A., & Chadimová, L. (2015). The middle and upper Lochkovian (Lower Devonian) conodont successions in key peri-Gondwana localities (Spanish Central Pyrenees and Prague Synform) and their relevance for global correlations. *Terra Nova*, *27*(6), 409–415. https://doi.org/10.1111/ter.12172

Valenzuela-Ríos, J. I., Liao, J.-C., & Martínez-Pérez, C. (2017). *The Devonian in the Compte sections* (pp. 89–91). Valencia: International Conodont Symposium 4. Progress on Conodont investigation.

Vorontsova, T. N., & Kuzmin, A. V. (1984). The Distribution of New Conodont Species of the Genus *Polygnathus* in the Famennian Deposits of Central Kazakhstan. *Izvestija Akademii Nauk SSSR, Ser. Geol.*, *10,* 58–64.

Walliser, O. H. (1996). Global Events in the Devonian and Carboniferous. In O. H. Walliser (Ed.), *Global Events and Event Stratigraphy in the Phanerozoic* (pp. 225–250). Berlin: Springer. https://doi.org/10.1007/978-3-642-79634-0_11

Yazdi, M. (1999). Late Devonian–Carboniferous conodonts from Eastern Iran. *Rivista Italiana di Paleontologia e Stratigrafia*, *105*(2), 167–200.

Zhang, X., Over, D. J., Ma, K., & Gong, Y. (2019). Upper Devonian conodont zonation, sea-level changes and bio-events in offshore carbonate facies Lali section, South China. *Palaeogeography, Palaeoclimatology, Palaeoecology*, *531*, 109219. https://doi.org/10.1016/j.palaeo.2019.05.041

Ziegler, W. (1959). Conodonten aus Devon und Karbon Südwesteuropas und Bemerkungen zur bretonischen Faltung (Montagne Noire, Massiv Mounthoumet, Span. Pyrenäen). *Neues Jahrbuch für Geologie und Paläeontologie, Monatshefte*, *7*, 289–309.

Ziegler, W. (1962a). Taxionomie und Phylogenie Oberdevonischer Conodonten und ihre stratigraphische Bedeutung. *Abhandlungen des Hessisches Landesamt für Bodenforschung 38*, 1–166.

Ziegler, W. (1962b). Die Conodonten aus den Geröllen des Zechsteinkonglomerates von Rossenray (südwestlisch Rheinberg/Niederrhein). *Fortschritte in der Geologie von Rheinland und Westfalen*, *6*, 391–406.

Ziegler, W., & Huddle, J. W. (1969). Die *Palmatolepis glabra*-Gruppe (Conodonta) nach der Revision der Typen von Ulrich & Bassler durch JW Huddle. *Fortschritte in der Geologie von Rheinland und Westfalen*, *16*, 377–386.

Ziegler, W., & Sandberg, C. A. (1984). *Palmatolepis*-based revision of upper part of standard Late Devonian conodont zonation. *Geological Society of America*, *Special Paper*, *196*, 179–194. https://doi.org/10.1130/SPE196-p179

Ziegler, W., & Sandberg, C. A. (1990). The Late Devonian Standard Conodont Zonation. *Courier Forschungsinstitut Senckenberg*, *121*, 1–115.

Zwart, H. J. (1979). The geology of the Central Pyrenees. *Leidse Geologische Mededelingen*, *50*(1), 1–74.